

## Comparative Study of Reversal Times of the Magnetization in Ferromagnetic and Antiferromagnetic Nanoparticles

Bachir Ouari

Department of Physics, Faculty of Sciences, la rocade, University of Tlemcen, Algeria

### ABSTRACT

We study the reversal times of the macrospine in individual ferromagnetic and antiferromagnetic nanoparticles by using matrix continued fraction method. It's shown that, at a high damping regime and at the small barrier, the behavior the relaxation of the magnetization in the ferromagnetic is similar to those for antiferromagnetic nanoparticle.

### \*Corresponding author

Bachir Ouari, Department of Physics, Faculty of Sciences, la rocade, University of Tlemcen, Algeria; E-Mail: ouari.univ@gmail.com

Received: May 17, 2021; Accepted: May 26, 2021; Published: June 10, 2021

### Introduction

There is currently intense interest in the use of nanoparticles for a wide range of biomedical and technological applications like the magnetic storage of information which is one of the essential elements high performance computers. Data exchange request switching of magnetization of magnetic storage cells (reversal of magnetization). And this is based on the deep knowledge of the magnetization reversal time, but this reversal time and with the technology currently used is of the order of nanosecond. If we want to have a more efficient computer (modern electronic computers run on a clock speed of the order of GHz). So quickly the reversal of the magnetization must be of great importance for the advancement of the high-speed information industry. The reversal of a magnetization can be obtained by different processes, and it is a tedious procedure but recent advances in technology allows us to manufacture magnetic nanoparticles which are considered useful for high density information storage [1-5]. For a magnetic nanoparticle, the magnetic moments of all atoms are normally aligned in the same direction, creating a so-called simple magnetic field. Such a nanoparticle is generally called Stoner-Wohlfarth or Stoner particle [6, 7]. Comprehension reversal of the magnetization of a single magnetic domain should be relatively simple in comparison to that of a loose system, but important in nanotechnology. *Ferromagnetic* nanoparticles are characterized by an internal potential, which may have several local equilibrium states with potential barriers between them. If the particles are small ( $\sim 100\text{\AA}$ ) so that these barriers are relatively low, the magnetization may escape from one potential well to another due to thermal agitation [8]. The ensuing thermal instability of the magnetization results in the phenomenon of superparamagnetism, because each fine particle behaves like an enormous paramagnetic atom having a magnetic moment  $\sim 104 - 105$  Bohr magnetons [9]. Nanoparticle that possess ferromagnetism have aligned atomic magnetic moments of equal magnitude, and their crystalline structures allow for direct coupling interactions between the moments, which may strongly enhance the flux density (e.g., Fe,

Ni, and Co). Furthermore, the aligned moments in ferromagnetic materials can confer a spontaneous magnetization in the absence of an applied magnetic field. Materials that retain permanent magnetization in the absence of an applied field are known as hard magnets. For the *antiferromagnetic* nanoparticles, the dynamics of the magnetization may differ in many respects from those of ferromagnetic nanoparticles because of the intrinsic properties of antiferromagnetic materials. Moreover, the magnetic behavior of antiferromagnetic nanoparticles can be quite different from that observed in the bulk, e.g., enhanced magnetic moment and coercivity, exchange bias, increase in magnetic moment with temperature, decrease in the susceptibility with temperature below the ordering (Néel) temperature  $T_N$  and its enhancement compared to that in bulk. The basic theory of antiferromagnetic nanoparticles was developed by Néel, who concluded that the total magnetic compensation of the sub lattices in antiferromagnetic nanoparticles is not possible for a number of reasons, namely, unequal numbers of spins in crystal planes, spin frustration near the surface, lattice defects, etc [8]. Hence, an equilibrium magnetization should ensue in such particles, moreover, they should become super paramagnetic at a finite temperature just as ferromagnetic nanoparticles. According to Néel's theory, "superantiferromagnetism" is manifested in a nanoparticle that contains an even number of sub-lattice planes, which induces a slight increase in transverse susceptibility compared to that of a large sample size [8]. It should be noted that measurements on ferritin and ferrihydrite have shown that the apparent effective susceptibility of these particles is significantly two to three times greater than that of a microcrystal. The effective spontaneous magnetization of antiferromagnetic nanoparticles varies from several tenths to several Gauss units, i.e. it is of the same order of magnitude as the magnetization of weak ferromagnets. The initial theory of thermal fluctuations of the magnetization of fine magnetic particles due to Néel was further developed by Brown using the theory of stochastic processes [10]. At temperatures much lower than  $T_N$ , this theory may be adapted to antiferromagnetic

nanoparticles. In the simplest case, the magnetic moments of the sublattices  $\mathbf{u}_1$  and  $\mathbf{u}_2$  of an antiferromagnetic particle subjected to a dc magnetic field  $\mathbf{H}$  are given by

$$\mathbf{u}_{1,2} = \mathbf{n} \left[ \pm v M_S + \mu / 2 - v \chi_A (\mathbf{n} \cdot \mathbf{H}) / 2 \right], \quad (1)$$

where  $M_S$  is the sublattice magnetization in a bulk,  $\chi_A$  is the linear susceptibility of a particle of unit volume,  $\mathbf{n} = (\mathbf{u}_1 - \mathbf{u}_2) / \mathbf{u}$  is the unit vector along the decompensation magnetic moment  $\mathbf{u} = \mathbf{u}_1 - \mathbf{u}_2$ ,  $u = |\mathbf{u}|$  and  $v$  is the particle volume. As long as the applied field  $\mathbf{H}$  is much weaker than the exchange field, the only possible motion of the vector  $\mathbf{u} = \mathbf{u}_1 - \mathbf{u}_2$  is rotation. Thus in the context of the Brown model, the magnetization dynamics of uniaxial antiferromagnetic nanoparticles are similar to the rotations of Brownian particles in liquids and are governed by a Fokker-Planck equation for the probability density function  $W$  of  $\mathbf{M}$ , viz.[12],

$$2\tau_N \frac{\partial}{\partial t} W = L_{FP} W, \quad (2)$$

where  $L_{FP}$  is the Fokker-Planck operator, given in reference [12] and  $\tau_N$  is the free diffusion time of the magnetization given by

$$\tau_N = \beta u (1 + \alpha^2) / (2\gamma\alpha) \quad (3)$$

Where  $\beta = (kT)^{-1}$ ,  $k$  is Boltzmann's constant,  $T$  is the absolute temperature, and  $\alpha = \gamma\eta u$  is the dissipation parameter. Here the normalized free energy of the particle subjected to a dc magnetic field  $\mathbf{H}$  applied at an angle  $\psi$  to the easy axis of the magnetization is [15]

$$\beta V = \sigma \left[ \sin^2 \vartheta - 2h(\cos\psi \cos\vartheta + \sin\psi \sin\vartheta \cos\varphi) + 2\sigma h^2 \zeta (\cos\psi \cos\vartheta + \sin\psi \sin\vartheta \cos\varphi)^2 \right], \quad (4)$$

where  $\sigma = v\beta K$  is the dimensionless anisotropy parameter,  $K$  is the anisotropy constant,  $h = \zeta / (2\sigma)$  is the applied field parameter,  $\zeta = \beta u H$ , and  $\beta v \chi_A H^2 / 2$  is the "antiferromagnetic" parameter (without loss of generality it is supposed that the field  $\mathbf{H}$  is in the  $xz$  plane). Equation (4) is similar to that the equation governing the magnetization dynamics of uniaxial ferromagnetic particles and at  $\zeta = 0$  reduces to it. The free energy become [13]

$$\beta V = \sigma \left[ \sin^2 \vartheta - 2h(\cos\psi \cos\vartheta + \sin\psi \sin\vartheta \cos\varphi) \right] \quad (5)$$

The free energy per unit volume  $V$ , Eq.(5) has a bistable structure with two minima separated by a potential barrier with a saddle point . The saddle point is generally in the equatorial region, while the two minima lie in the north and south polar regions, respectively (see Fig. 1.a).

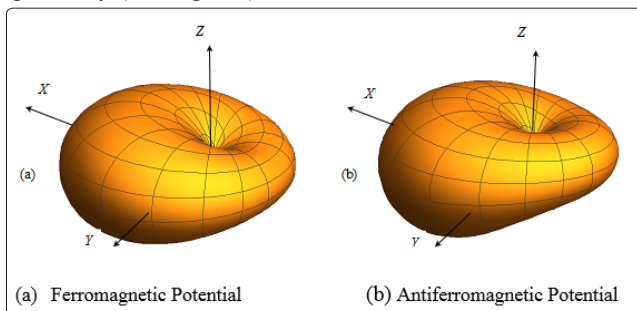


Figure 1: 3D plot of the potential Eq.(4) Eq.(5) for  $\sigma = 10$ ,  $h = 0.15$ ,  $\zeta = 0.15$ , and  $\psi = \pi/3$

Now the reversal time of the magnetization in magnetic nanoparticles is associated with the inverse of the smallest

nonvanishing eigenvalue  $\lambda_1$  of the Fokker-Planck operator  $L_{FP}$  in Eq. (2) characterizing the slowest overbarrier relaxation mode and, hence, the long-time behavior of the magnetization.

In this paper, we use the matrix continued fraction method given in reference to calculate the reversal time of magnetization of antiferromagnetic and ferromagnetic nanoparticles subjected to a continuous magnetic field applied at an arbitrary angle  $\psi$  with respect to the easy axis of magnetization. We then proceed to a comparative study of the two reversal times. The particular case of a DC magnetic field parallel to the easy axis, i.e.  $\psi = 0$ , has recently been examined by Raikher [14]. In relation to the low-frequency magnetodynamics of antiferromagnetic nanoparticles suspended in a fluid by means of a kinetic model of magnetization relaxation within the limit of high magnetic anisotropy.

### Numerical Calculation of Magnetization Reversal Times

The solution of the Fokker-Planck Eq. (2) is first reduced to an infinite hierarchy of differential-recurrence equations for the statistical moments  $c_{l,m}(t) = \langle Y_{l,m}[\vartheta(t), \varphi(t)] \rangle$  governing the magnetization relaxation, namely,

$$\frac{d}{dt} c_{l,m}(t) = \sum_{l',m'} d_{l',m',l,m} c_{l',m'}(t), \quad (6)$$

where  $d_{l',m',l,m}$  are the matrix elements of the Fokker-Planck operator in Eq. (2) and the angular brackets denote the statistical average. A method of derivation of Eq. (6) for arbitrary anisotropy potential is given in Refs. 5 and 6. Equation (6) can be transformed into the tridiagonal vector recurrence equation,

$$\frac{d}{dt} \mathbf{C}_n(t) = \mathbf{Q}_n^- \mathbf{C}_{n-1}(t) + \mathbf{Q}_n \mathbf{C}_n(t) + \mathbf{Q}_n^+ \mathbf{C}_{n+1}(t), \quad (7)$$

where  $\mathbf{C}_n(t)$  are the column vectors arranged in an appropriate way from  $c_{l,m}(t)$ , and  $\mathbf{Q}_n^-, \mathbf{Q}_n, \mathbf{Q}_n^+$  are the matrices with elements  $d_{l',m',l,m}$ . Equation (7) can be solved using matrix continued fractions. By solving Eq. (7) we have, in particular, the smallest non-vanishing eigenvalue  $\lambda_1$  of the Fokker-Planck operator which is associated with the slowest relaxation mode. All the method of calculation are given in Refs.5 and 6

### Results and Discussion

By way of illustration,  $\lambda_1$  calculated with the matrix continued fraction method as functions of the anisotropy (or the inverse temperature) parameter  $\sigma$  are shown in Figs. 2 various values of the model parameters  $h$  (external field parameter) and the damping. In Figs. 4,  $\lambda_1$  is plotted as a function of  $\psi$ . Figures 2 and 3 demonstrate that changes in the magnetic field parameter and in the antiferromagnetic parameter  $\zeta$  significantly affect the relaxation process. Namely as  $\zeta$  increases the reversal time decreases, which may be attributed to decrease of the effective anisotropy constant  $\sigma' = \sigma - \zeta^2/2$ . Thus, the variation of the model parameters affects strongly the reversal time of the magnetization leading to changes in the reversal time  $\tau$  of several orders of magnitude. Figures 5 illustrate the damping dependence of  $\lambda_1$  for various values of the external field  $h$ .

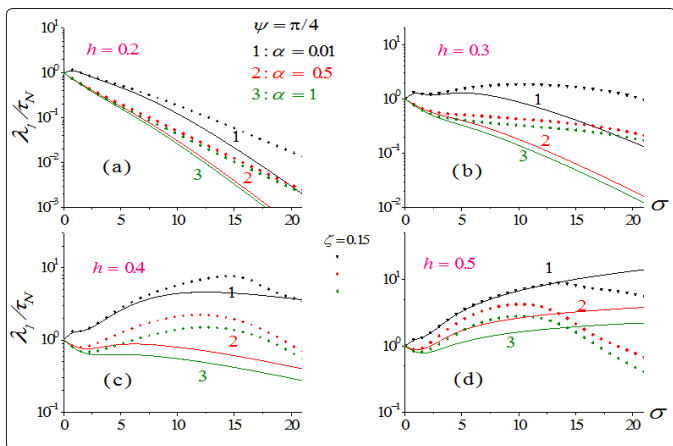


**Figure 2:**  $\lambda_1 \tau_N$  vs. the anisotropy (or the inverse temperature) parameter  $\sigma$  for  $\alpha = 0.01$ ,  $\zeta = 0.15$ ,  $\psi = \pi/4$ , and various values of the field parameter  $h$  and the damping  $\alpha = 0.01, 0.5, 1$ . Solid lines : ferromagnetic. Symbols: antiferromagnetic

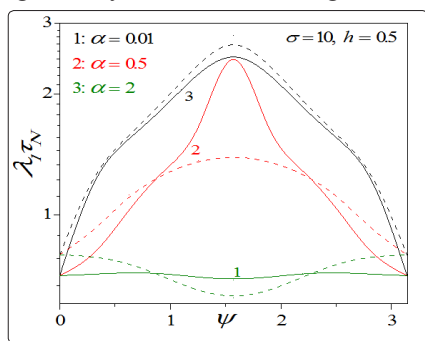


**Figure 3:**  $\lambda_1 \tau_N$  vs. the oblique angle  $\psi$  for  $\zeta = 0.15$ ,  $\sigma = 10$ ,  $h = 0.5$  and various values of the damping  $\alpha = 0.01, 0.5, 2$ . Solid lines : ferromagnetic. Symbols: antiferromagnetic

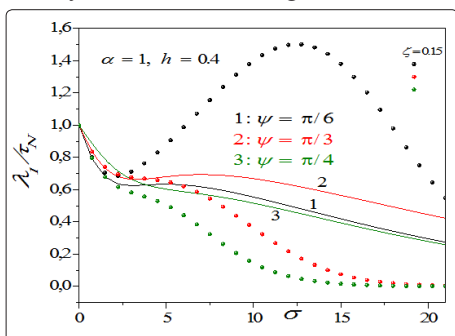


**Figure 4:**  $\lambda_1 \tau_N$  vs  $\sigma$  for  $h = 0.4$ ,  $\psi = \pi/4$ ,  $\alpha = 1$ , and various values of the antiferromagnetic parameter  $\zeta$ . Solid lines : ferromagnetic. Symbols: antiferromagnetic

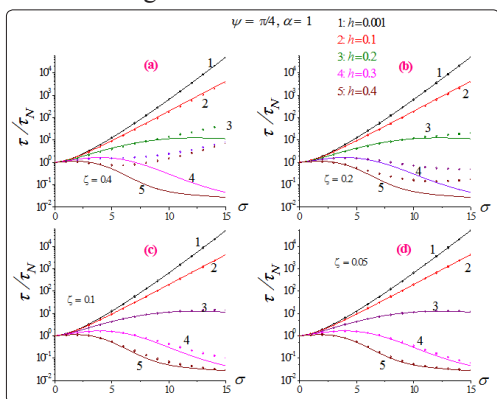


**Figure 5:**  $\lambda_1 \tau_N$  vs.  $\sigma$  for  $\zeta = 0.05, 0.1, 0.2, 0.4$ ,  $\psi = \pi/4$ ,  $\alpha = 1$ , and

various value of the field parameter  $h = 0.001, 0.1, 0.2, 0.3, 0.4$  and  $\alpha$ . Solid lines : ferromagnetic. Symbols: antiferromagnetic

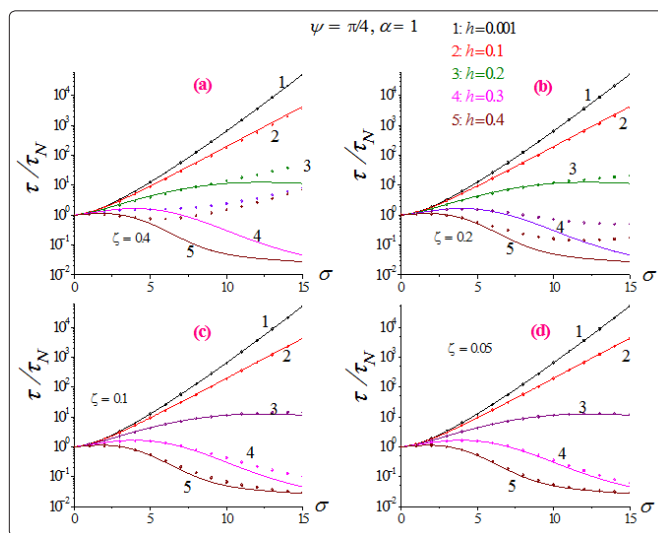


**Figure 6:**  $\lambda_1 \tau_N$  vs. the damping parameter  $\alpha$  for  $\zeta = 0.15$ ,  $\psi = \pi/4$ ,  $\sigma = 10$ , and various values of the field parameter  $h = 0.1, 0.15, 0.2, 0.25, 0.3$ . Solid lines : ferromagnetic. Symbols: antiferromagnetic

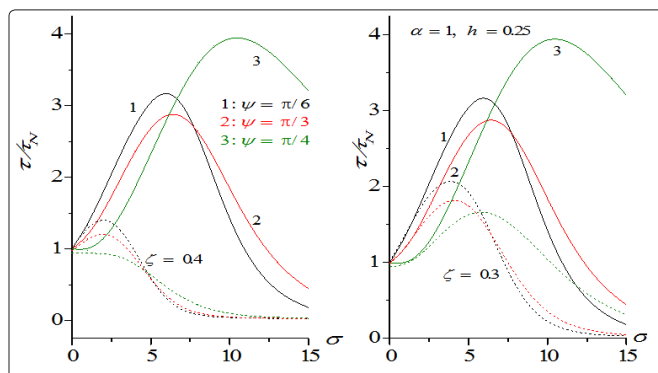


**Figure 7:**  $\lambda_1 \tau_N$  vs.  $\sigma$  for  $\psi = \pi/6, \psi = \pi/4, \psi = \pi/3$ ,  $\zeta = 0.3, 0.4$ ,  $\alpha = 1$ , and various value of the field parameter  $h = 0.25$ , Solid lines : ferromagnetic. Symbols: antiferromagnetic

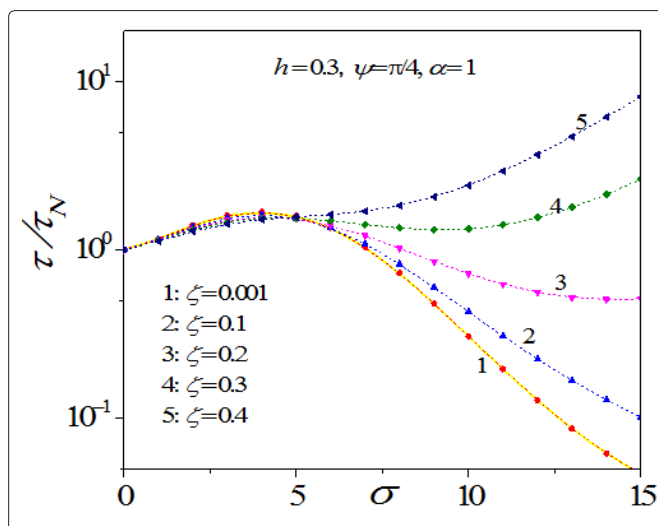


**Figure 8:**  $\lambda_1 \tau_N$  vs.  $\sigma$  for  $\psi = \pi/4$ ,  $\alpha = 1$ , and various value of the antiferromagnetic parameter  $\zeta = 0.001, 0.1, 0.2, 0.3, 0.4$ , field parameter  $h = 0.3$ , Solid lines : ferromagnetic. Symbols: antiferromagnetic

As is apparent from Fig. 5 the integral relaxation time  $\tau$  in the ferromagnetic nanoparticles may have a behavior dramatically different from that of the antiferromagnetic above certain critical values of the parameters, if  $h > h_c$ , the relaxation time has no longer Arrhenius-type behavior. At this critical value of  $h$ , the relaxation switches from being dominated by the slowest overbarrier mode to being dominated by the fast intrawell relaxation modes due to the depletion of population in the upper (shallow) well. The critical value  $h_c \approx 0.17$  so obtained coincides with that found by Garanin for uniaxial particles [16-19].

### Conclusion

The reversal times of the magnetization of the ferromagnetic and antiferromagnetic nanoparticles were investigated numerically. We demonstrated that at high damping regime and at the small barrier, the behavior the relaxation of the magnetization in the ferromagnetic is similar to those for antiferromagnetic nanoparticle.

We have evaluated the reversal time of the magnetization for antiferromagnetic nanoparticles subjected to a uniform external field  $H_0$  applied at an arbitrary angle  $\psi$  to the easy axis of the particle using the model suggested by Raikher et al. Our results can be used to study stochastic resonance and dynamic hysteresis in antiferromagnetic nanoparticles which may differ essentially from those in fine ferromagnetic particles. For the particular case,  $\psi = 0$ , our results entirely agree with those reported by Raikher et al. It should be noted that in this study, surface effects and particle interactions were ignored. These constraints cause great mathematical difficulties in the formulation of a realistic theoretical model. However, they can, in principle, be controlled in the interpretation of experimental data by varying the size of the particles and concentrations.

### Acknowledgments

We thank Prof. William T Coffey, Professor H. Aourag director of research and development in Algeria, for useful comments.

### References

1. Robert C. O'handley, Modern Magnetic Materials: Principles and Applications, (John Wiley & Sons, New York, (2000).
2. Shouheng Sun, C. B. Murray, D. Weller, L. Folks, and A. Moser, Science 287, 1989 (2000).
3. C. T. Black, C. B. Murray, R. L. Sandstrom, and Shouheng Sun, Science 290, 1131 (2000).
4. S. I. Woods, J. R. Kirtley, Shouheng Sun, and R. H. Koch, Phys. Rev. Lett. 87, 137205 (2001).
5. D. Zitoun, M. Respaud, M.-C. Fromen, M. J. Casanove, C. Amiens, and B. Chaudret, Phys. Rev. Lett. 89, 037203 (2002), Carvalho, M.D.; Henriques, F.; Ferreira, L.P.; Godinho, M.; Cruz, M.M, J. Solid State Chem., 201, 144–152 (2013)
6. E. C. Stoner, and E. P. Wohlfarth, Phil. Trans. Roy. Soc. London A.240, 599 (1948), reprinted in IEEE Trans.29 Magn. 27, 3475 (1991).
7. Z. Z. Sun and X. R. Wang, 10.1103/Phys. Rev.B.73. 092416 (2006)
8. L.Néel, Ann. Géophys. 5, 99 (1949).
9. C. P. Bean and J. D. Livingston, J. Appl. Phys. Suppl. 30, 120S (1959).
10. M. S. Seehra and A. Punnoose, Phys. Rev. B 64, 132410 (2001), Yu. L. Raikher and V. I. Stepanov, J. Exp. Theor. Phys. 107, 435 (2008) [Zh. Eksp. Teor. Fiz. 134, 514 (2008)]
11. W. F. Brown, Jr, Phys. Rev. 130, 1677 (1963).
12. W. T. Coffey, Yu. P. Kalmykov, and J. T. Waldron, The Langevin Equation, 2nd Ed. (World Scientific, Singapore,

- 2004).
13. Yu. P. Kalmykov, J. Appl. Phys. 96, 1138 (2004).
14. Yu. P. Kalmykov and B. Ouari, Phys. Rev. B 71, 094410 (2005); Yu. P. Kalmykov, W.T. Coffey, B. Ouari, and S. V. Titov, J. Magn. Mater. 292, 372 (2005), B. Ouari and Yu. P. Kalmykov, J. Appl. Phys. 100, 123912 (2006); Yu. P. Kalmykov, J. Appl. Phys. 101, 093909 (2007);
15. B. Ouari, S. Aktaou, and Yu. P. Kalmykov, Phys. Rev. B 81, 024412 (2010).
16. W. T. Coffey, D. S. F. Crothers, J. L. Dormann, L. J. Geoghegan, and E. C. Kennedy, Phys. Rev. B 58, 3249 (1998).
17. Yu. L. Raikher, V. I. Stepanov, A. N. Grigorenko, and P. I. Nikitin, Phys. Rev. E 56, 6400 (1997); Y. L. Raikher and V. I. Stepanov, Phys. Rev. Lett. 86, 1923 (2001).
18. Yu. L. Raikher, V. I. Stepanov, and R. Perzynski, Physica B 343, 262 (2004).
19. D. A. Garanin, E. C. Kennedy, D. S. F. Crothers, and W. T. Coffey, Phys. Rev. E 60, 6499 (1999).

**Copyright:** ©2021 Bachir Ouari. This is an open-access article distributed under the terms of the Creative Commons Attribution License, which permits unrestricted use, distribution, and reproduction in any medium, provided the original author and source are credited.